Michael Baker INTERNATIONAL

"… the strength of the Pack is the Wolf, and the strength of the Wolf is the Pack…"

Evaluation and Retrofit of Steel Girder Shiplap Connections

B. Kozy
Michael Baker International, Baltimore, MD

J. Beckstrom & T. Armbrecht
Michael Baker International, Chicago, IL

Written with cooperation of the Illinois Department of Transportation
Bureau of Bridges and Structures, Springfield, IL

ABSTRACT: Over time, owners may face challenges with management of bridges with outdated details. One such detail that is no longer used today is the steel girder shiplap connection. These were originally employed to simplify analysis of continuous girders while also moving joints away from the piers, improving longevity of bridge bearings and substructures. Unfortunately, fatigue issues have appeared in these connections resulting in cracking at critical load-carrying locations. In this project, analysis was performed to investigate connection fatigue and strength and retrofit design verification. Results utilizing non-linear analysis showed that while stresses from ultimate loading could adequately redistribute throughout the web, high stress concentrations were created, exacerbating fatigue. Stress calculations for shiplap web details are not well codified or easily assessed with simple hand calculations, so finite element analysis was utilized. Results showed web fatigue life had been exhausted with more cracking expected at other locations, convincing the owner retrofit was necessary even though the bridge was programmed for replacement.

1 BACKGROUND

The Chain of Rocks Bridge is a 43-span continuous, cantilevered steel girder bridge constructed in 1966 just north of Granite City, IL that carries I-270 East Bound (EB) and West Bound (WB) over the Mississippi River. See Figure 1 for bridge general elevation. The bridge has separate, parallel superstructures for EB and WB that share a single substructure and are composed of continuous two-girder units with cantilever and suspended spans with hinges created by shiplap connections. See Figure 2 for typical shiplap connection. In total, there are 12 shiplap girder connections. Michael Baker International (MBI) was contacted by the Illinois Department of Transportation (IDOT) regarding a crack found at the end of the tapered web of one the shiplap hinge connections that was arrested with a 21mm (13/16") drilled hole performed by IDOT previously. See Figure 3. The crack initiated at a sharp discontinuity in the web plate end, where the plate transitioned from vertical to sloped geometry. It was determined that detailed analysis was needed to verify the safe load capacity of the connection, ensure no immediate safety concern existed, and determine any need for remedial actions. Additionally, many similar web imperfections also existed in the other shiplap connections due to previous flame cutting around the end of the tapered web. See Figure 4. Fatigue evaluation as well as strength evaluation of the shiplap connections was deemed necessary for the various web geometries. There were additional concerns since the girders were known to contain 690MPa (100ksi) "T-1" steel which was a primary cause of the major fracture that occurred on the Hernando de Soto Bridge between Tennessee and Arkansas in 2021. IDOT had programmed this bridge for replacement within five years and considered the option of monitoring the uncracked ship-lap locations at a three-to-six-month frequency instead of retrofitting. However, due to the high volume of traffic using the structure, the lack of redundancy, and the relative ease to install innovative retrofit details developed by MBI, retrofits were installed at all accessible locations.

Figure 1. General elevation of the bridge. (Courtesy of IDOT)

Figure 2. Typical As-designed shiplap connection.

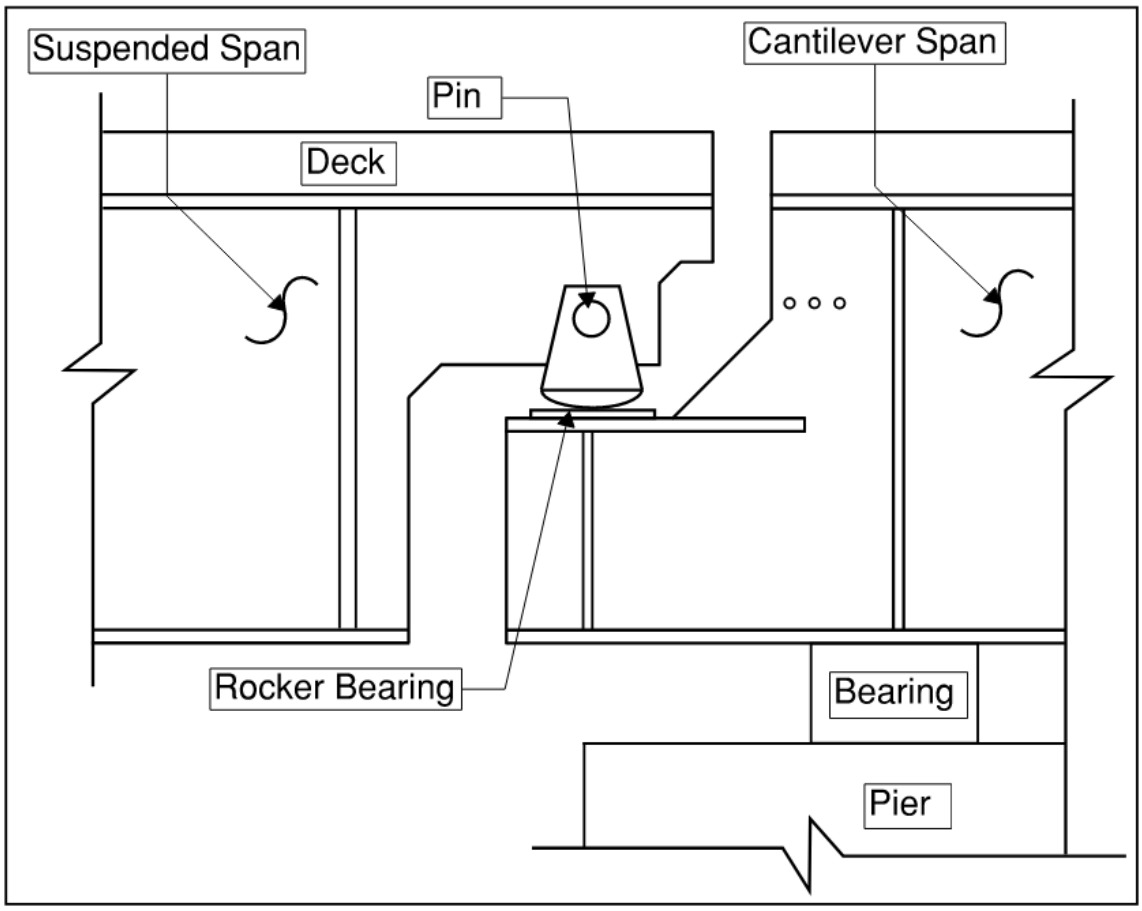

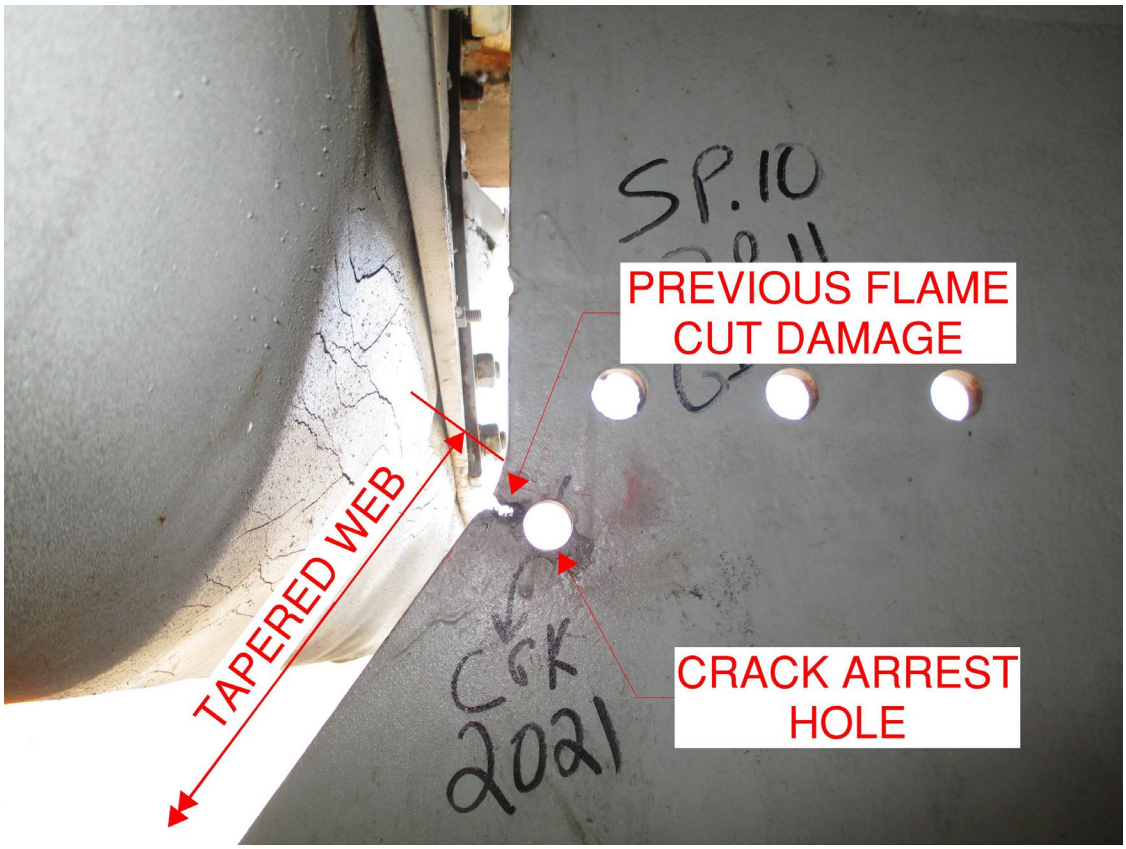

Figure 3. Photo of Crack Location with crack arrest hole drilled at tip of crack.

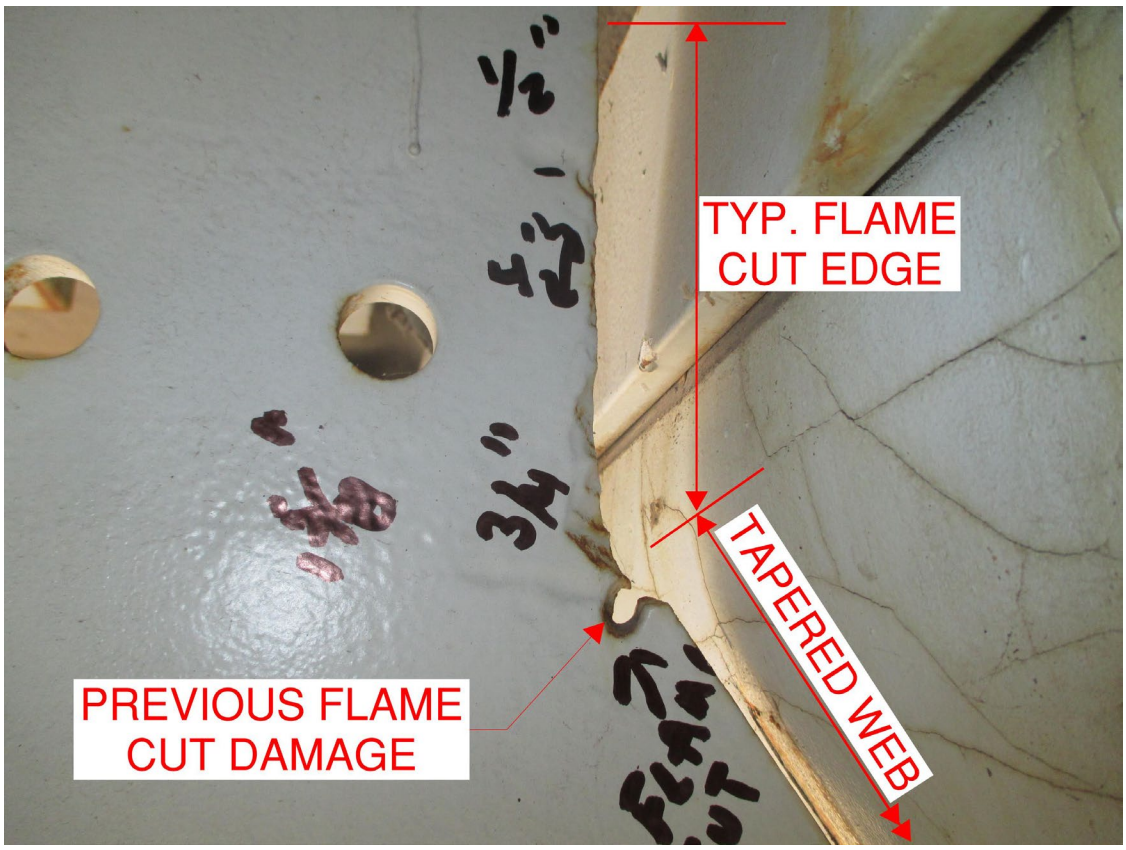

Figure 4. Typical flame-cut edge and flame-cut damage at end of tapered web.

2 INSPECTION

IDOT requested MBI to perform additional in-depth inspections to verify the crack arrest hole captured the tip of the crack and look at other locations of the shiplap connection detail. The Under Bridge Inspection (UBI) vehicle provided by IDOT allowed hands on access to both girders of the westbound structure and the north girder of the eastbound structure. The south girder of the eastbound structure was visually inspected from a distance due to difficulties in achieving access. Inspections included both visual and Magnetic Particle Testing (MT) to determine the presence of fatigue cracks. No additional crack indications were noted during these in-depth inspections. Table 1 shows a summary of the inspection findings at all the shiplap connections.

Table 1. Summary of inspection findings near tapered web.

	Girder 1	Girder 2	Girder 3	Girder 4
Pier 7	No defects	Undercut weld	No defects	No defects
Pier 11	Crack arrest hole	Flame-cut gouge	Gouge	No defects
Pier 15	Flame-cut gouge	No defects	Flame-cut gouge	No defects
Pier 19	Flame-cut gouge	Flame-cut hole	No defects	No defects
Pier 24	Gouge	Flame-cut gouge	Flame-cut gouge	No defects
Pier 28	No defects	Notch	No defects	No defects

3 REPAIR DETAIL DEVELOPMENT

MBI proceeded to develop repair concepts immediately based on the observed fatigue damage and data collected from the in-depth inspections. Even prior to any analysis, it was clear that the cracked location needed further repair and strengthening, and the irregular geometry of the web free edge at other locations would create many potential sites for additional fatigue crack initiation if not mitigated. It was unknown why the edge geometry was in the observed condition, but it was speculated that a cut was made to provide additional clearance for the expansion joint trough. Of particular concern was that these connections all provide a primary load path in a structural member classified as a nonredundant steel tension member, NSTM (previously called fracture critical member). The unique concern with this detail is that any crack growth is not self-arresting, but rather will accelerate to possible collapse if the progression is not detected in time.

Preliminary fatigue assessment using detailed finite element analysis indicated that live load stresses were very high at the location where cracking was observed; well above the fatigue threshold specified in AASHTO LRFD for base metal at free edges of structural steel members. This both confirmed that the cracking was expected at this location, and also raised the concern that other similar details would also be at risk of similar fatigue cracking.

The development of the repair concept started by investigating geometric improvements that could be made to reduce the stress concentration at the location of interest. Options to cut away material and increase the radius at the slope transition point were explored with some success. Changing the web end geometry by cutting had the added benefit of removing any material with existing fatigue damage that may be “on the cusp” of developing visible crack growth. Essentially, it would “reset” the fatigue life clock. However, the stresses could not be reduced sufficiently below the threshold by geometry improvements alone. Supplemental thickness was needed to achieve sufficient reductions in stress range. The desire was to achieve infinite life with the retrofit, if possible. In the development of the repair concept, consideration needed to be given to many factors including:

- Repairs were to be completed while bridge was open to routine traffic.
- IDOT skilled maintenance labor was to be utilized.
- Minimize material removal for additional bolt holes and web reprofiling.
- Web edge inspectability after repairs.

The final retrofit concept included a combination of geometry improvements to the web end, grinding, and adding two new stiffening (strap) plates, which were bolted to the web across the region of high stress. To minimize web material removal the details utilized two of the three

existing web bolt holes from previous joint trough supports for the repair plates connections. The retrofit also incorporated a "viewing window" in the repair plates to allow web edges to be inspected as desired. The detail concept was shared with IDOT maintenance staff to ensure they could make web repairs, fabricate plates, and install them with their current workforce and capability. The final reprofiling repair detail (at all locations other than the crack arrest hole) as well as the repair plate installation detail are shown in Figures 5 and 6. Field completed examples of the repair at the crack arrest hole and a typical reprofiling location are shown in Figures 7 and 8. The web reprofiling repair included several steps for the IDOT maintenance staff to follow:

- Reprofiling to be completed using plasma cutting leaving a minimum of 6mm (¼") of material remaining to the final profile.
- The 6mm (¼") of excess material to be ground smooth with a die grinder with carbide rotary burr tip to a roughness average (Ra) of 6µm (250µin) or less.
- Ground surfaces to be inspected for cracks using magnetic particle testing after completion.

Figure 5. Detailed repair plan detail for web reprofiling to 102mm (4") radius up to 25mm (1") deep into base metal.

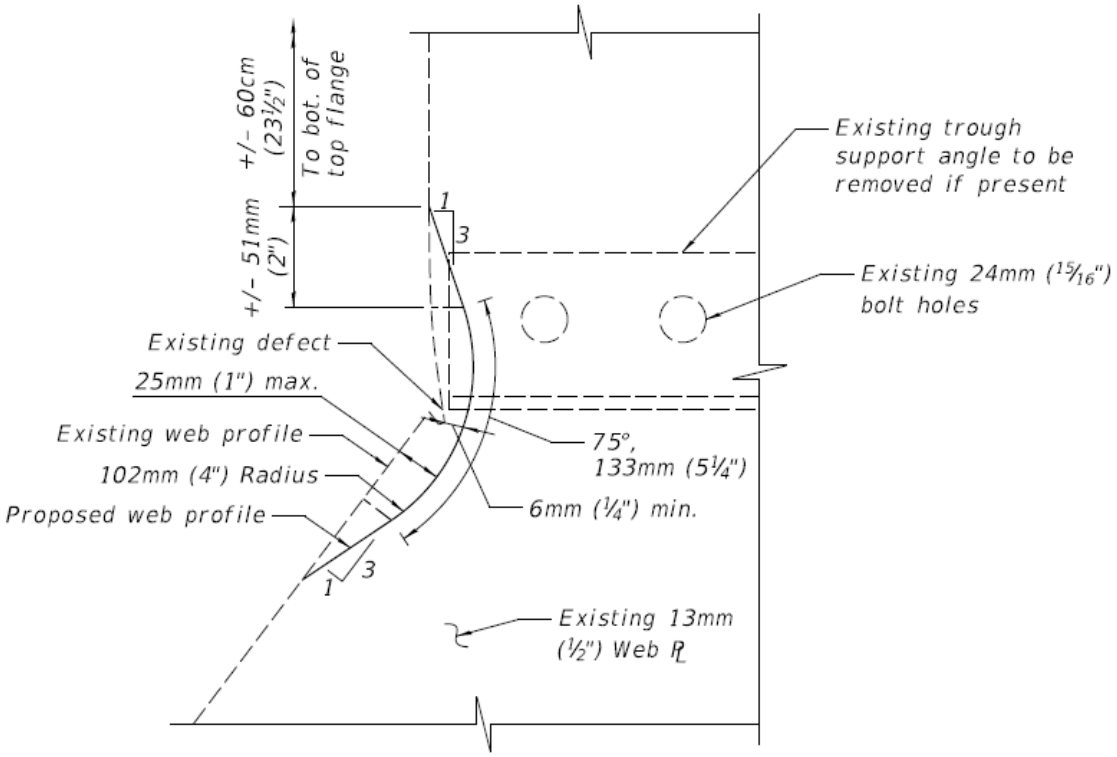

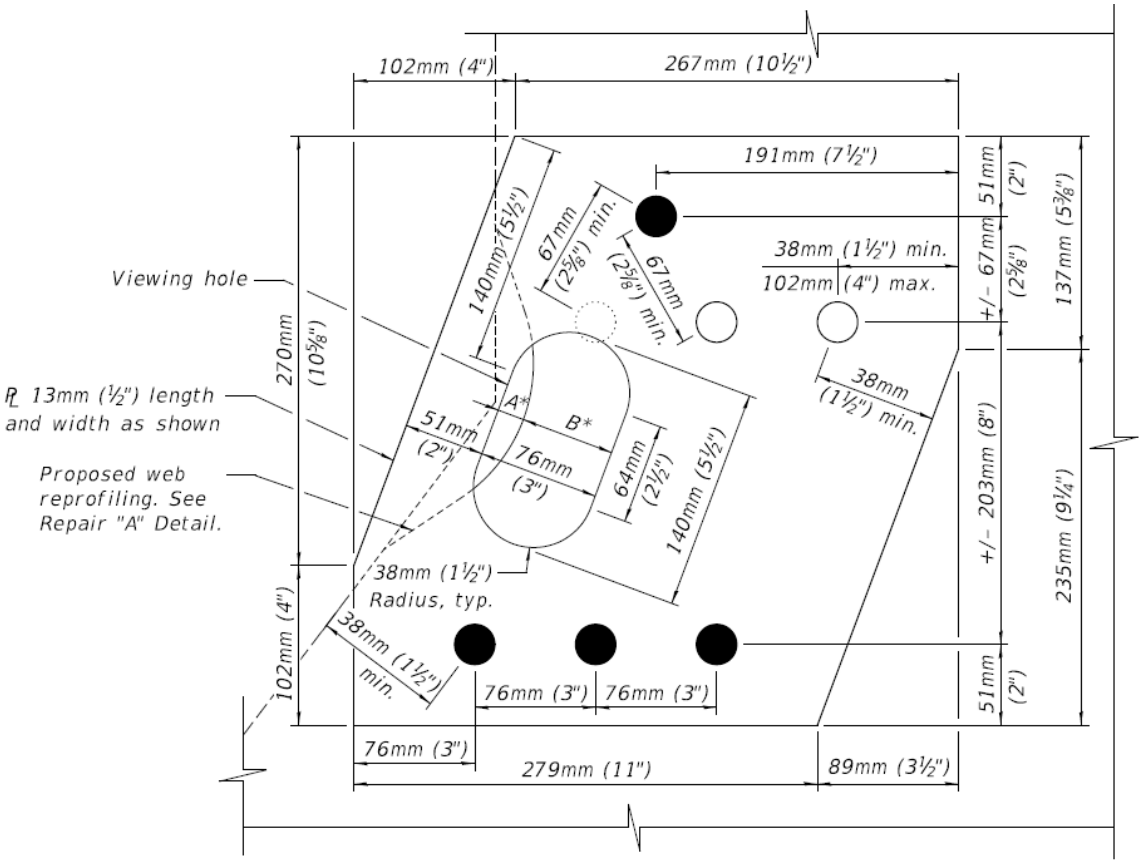

Figure 6. Detailed repair plan detail for installation of strap plates on both sides of the web.

Figure 7. Final repair at arrest hole location (plate on opposite side not visible). (Courtesy of IDOT)

Figure 8. Final typical repair at web reprofiling (plate on opposite side not visible). (Courtesy of IDOT)

4 FATIGUE EVALUATION

4.1 *Basis of Evaluation*

The basis of the fatigue assessment is the *AASHTO LRFD Bridge Design Specifications* [1] and the *AASHTO Manual for Bridge Evaluation* [2] with some additional interpretations necessary to utilize results from a refined three-dimensional finite element analysis model which are described in the Federal Highway Administration's (FHWA) *Design and Evaluation of Steel Bridges for Fatigue and Fracture*. [3] The assessment assumes a category A fatigue detail resistance, corresponding to section 1.1 in Table 6.6.1.2.3-1 in AASHTO LRFD, since the existing web edge will be cut to a new geometry profile and ground smooth as part of the repairs. A category A fatigue detail utilizes an A-constant equal to 82×10^{11} MPa^3 (250×10^8 ksi^3) and a constant-amplitude fatigue threshold (allowable fatigue stress range for more than 2 million cycles) equal to 165MPa (24ksi). The stress range cycles (n) per truck is assumed to be 1.0 since the cantilever is so short and the stress range is dominated by loading on the suspended span (not the cantilever). [1] Additionally, the MBE factors Rp and Rs per Section 7.2.2.1 are included to modify the finite fatigue stress ranges based on multiple presence and fatigue-life evaluation methods, respectively. The Rs factor used is 0.90 since refined analysis is used for determining fatigue stress ranges. [2] The 2019 single-lane Average Daily Truck Traffic (ADTT) of 4170 is used for all calculations. This value is conservatively used throughout the evaluation although recent traffic data would suggest this value could be decreased. The recent traffic data based on highway cameras showed approximately a 7% reduction in ADTT while Weight-In-Motion (WIM) data showed approximately a 6% increase in ADTT with a 22% decrease in truck weight. Although the recent traffic data was provided, it did not come with an adequate amount of confidence to be considered for the analysis.

Fatigue assessment was performed for the web end taper area of the cantilever girders for the original "as-designed" condition as well as in the damaged condition from subsequent flame cutting and the arrested crack condition. Fatigue stress ranges due to the AASHTO fatigue truck were taken at the free edge of the web, 6mm (¼") away from the edge, and 13mm (½") away from the edge. As recommended for checking the free edge of cutout regions in orthotropic steel decks, [4] the location for selecting the fatigue stress range to assess the fatigue life of each detail can be taken at 1/2t or 6mm (1/4") from the edge due to the steep stress gradient at the free edge. This stress gradient and the offset limits are shown in Figure 9. Stresses were taken at tangential orientation to the plate edges, since this is the direction of stress that would initiate and propagate a crack at the free edge.

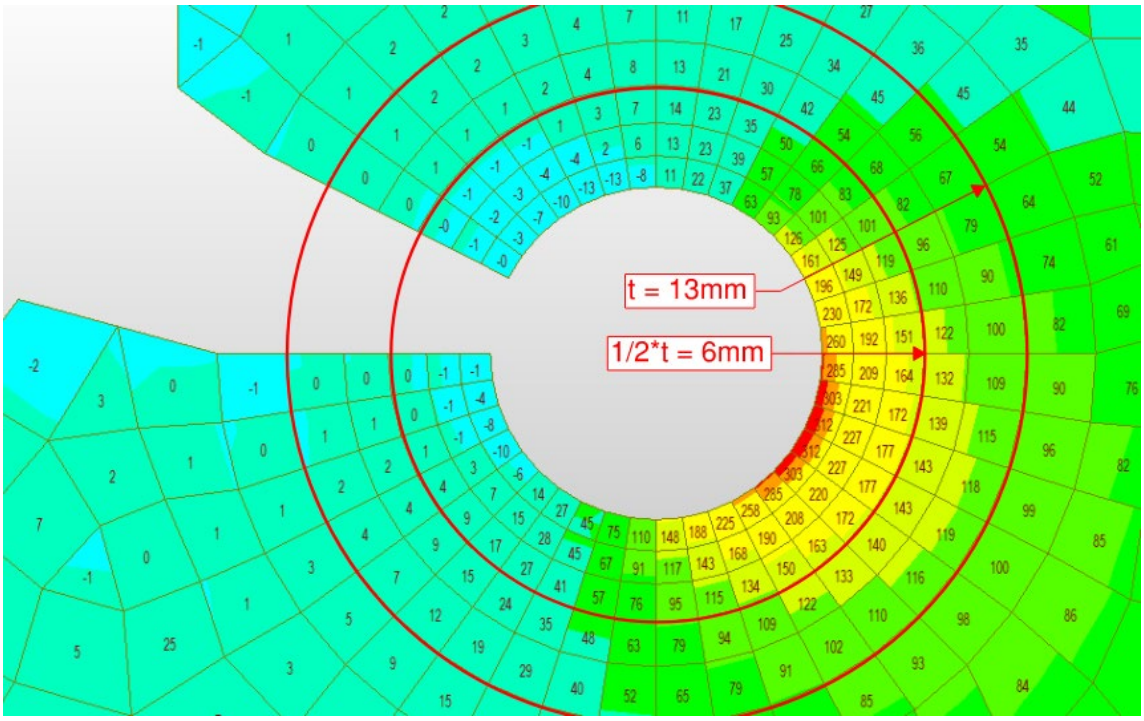

Figure 9. Fatigue stress gradient and offset limits at location with crack and arrest hole (MPa).

The stress ranges were multiplied by 1.75 and compared against the constant-amplitude fatigue threshold to determine whether infinite fatigue life could be achieved. If the stress multiplied by 1.75 was greater than the fatigue threshold, then the detail could only withstand a finite number of load cycles, N, based on the stress range multiplied by 0.8. Load cycles are determined as $N = (365)(\text{years})(n)(ADTT)_{SL}$ per LRFD Eq. 6.6.1.2.5-3. The effective stress range, $(\Delta F)_n = R_p R_s \Delta f$, is estimated per MBE Eq. 7.2.2-1 using the stress range, Δf, multiplied by 0.8. Plugging N and $(\Delta F)_n$ into the stress range equation, $(\Delta F)_n = (A/N)^{(1/3)}$, per LRFD Eq. 6.6.1.2.5-2 [1] and rearranging to solve for "years" from the load cycle equation provides a way to calculate the fatigue life based on the fatigue stress range.

4.2 *Modeling Details*

The finite element models were developed in Midas Civil using plate elements for the girder web, flanges, and stiffeners and solid elements for the haunch and effective width of concrete deck. It is widely accepted throughout the industry that plate elements are adequate to characterize the local effects of structures made up of relatively thin material with minimal effect in the through-thickness direction. [3] The cantilever section of the girder was braced laterally where transverse members framed in. The length of girder modeled was determined through incremental increases in length and was chosen when an increase in length had no further influence on stresses in the cantilever section of the girder. Mesh size in the web taper was kept approximately equal to the 13mm (½") web thickness consistent with LRFD modeling requirements for Level 3 design of

orthotropic steel decks, and gradually increased to 51mm (2”) away from the region of interest. [4] The fatigue analysis was run using linear elastic materials to determine maximum stress ranges due to a single HS-20 (equivalent to HL-93 in LRFD) fatigue truck. The model loading was applied at the center of the cantilever span rocker bearing, and its magnitude was equivalent to the fatigue truck reaction at the suspended span pin (extracted from the BrR model) factored for finite fatigue loading (0.8*L).

To get a baseline for the fatigue stress ranges, a model with the as-designed web was evaluated and compared to a model with the crack and arrest hole fully modeled as well as an idealized flame-cut gouge utilizing a 6mm (¼”) radius at its tip. After initial fatigue evaluation, these models were also compared to the stress ranges of various reprofiled webs with much larger radii and models with various repair plate configurations. The repair plates were modeled as plate elements and connected to the web with elastic rigid links at the locations where bolts would be used to fasten them together.

4.2.1 *Cantilever Span Web Region As-Designed Geometry*

In this model, the web taper corner is modeled with a 6mm (¼”) radius which equates to four (4) elements with an edge distance about 1mm (1/32”). This radius is added as an attempt to characterize the stress field at this corner. Figure 10 shows the corner geometry and maximum element stresses for the fatigue II stress range due to the LRFD fatigue truck in the linear-elastic model. The red boundary in Figure 10 shows the offset location 6mm (¼”) from the edge. This corresponds to the stress in the fourth row of nodes, and the sixth row of nodes corresponds to the stress range 13mm (½”) from the edge.

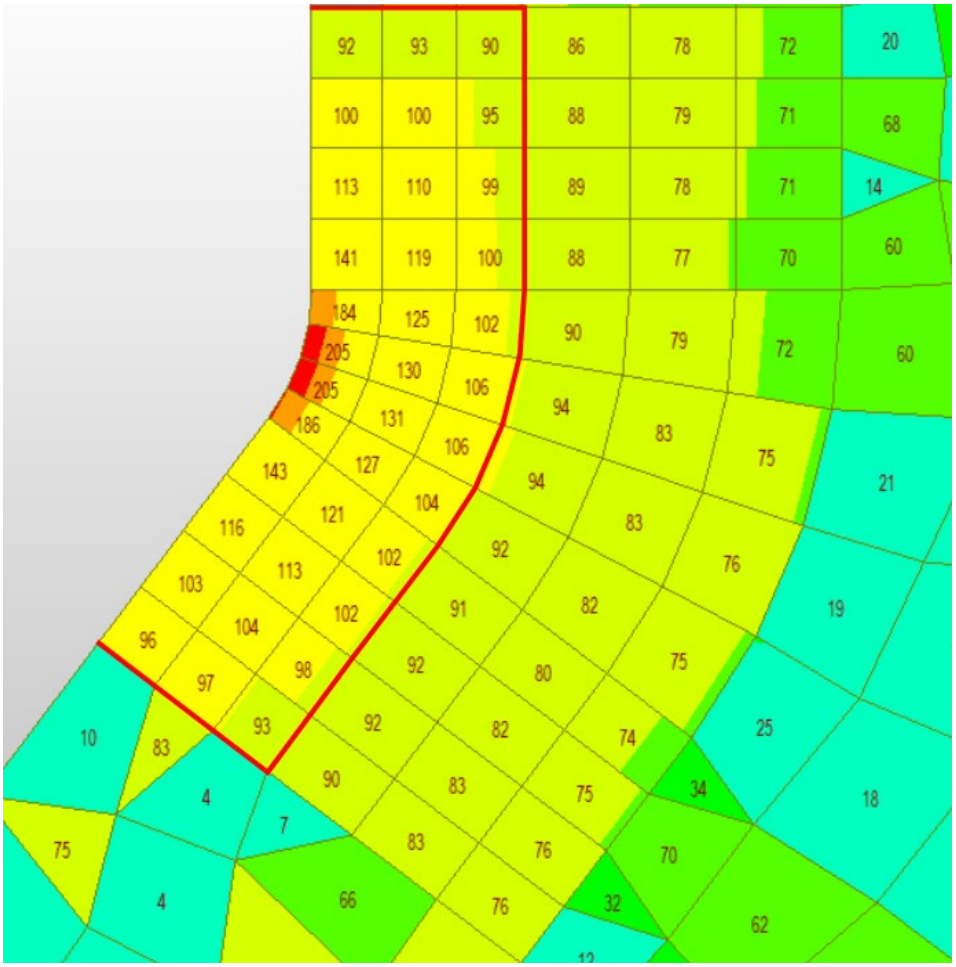

Figure 10. As-designed geometry, fatigue II maximum element local tangential stress Range (MPa).

4.2.2 *Cantilever Span Web Taper Region Flame-Cut Gouge Geometry*

In this model, the web taper corner is modeled with a 19mm (¾") deep gouge just below the corner to represent the flame cut damage that currently exists at some of these transition areas. A gouge radius of 6mm (¼") is the minimum that can be accurately analyzed in MIDAS due to mesh size limitations. Any smaller radius will not be able to effectively define the stress concentrations with the appropriate amount of edge elements. A geometry including the crack cannot be modeled because FEA will require an assumed radius for crack tip for accurate results, and the minimum allowable radius is already used in the gouge geometry. The gouge is modeled with a 9-degree angle between adjacent elements. Figure 11 shows the gouge geometry maximum element stresses for the fatigue II stress range due to the LRFD fatigue truck in the linear-elastic model. The red boundary in Figure 11 shows the location 6mm (¼") from the edge. The red boundary in Figure 12 shows the location 6mm (¼") from the edge. This corresponds to the stress in the fourth row of nodes, and the sixth row of nodes corresponds to the stress range 13mm (½") from the edge.

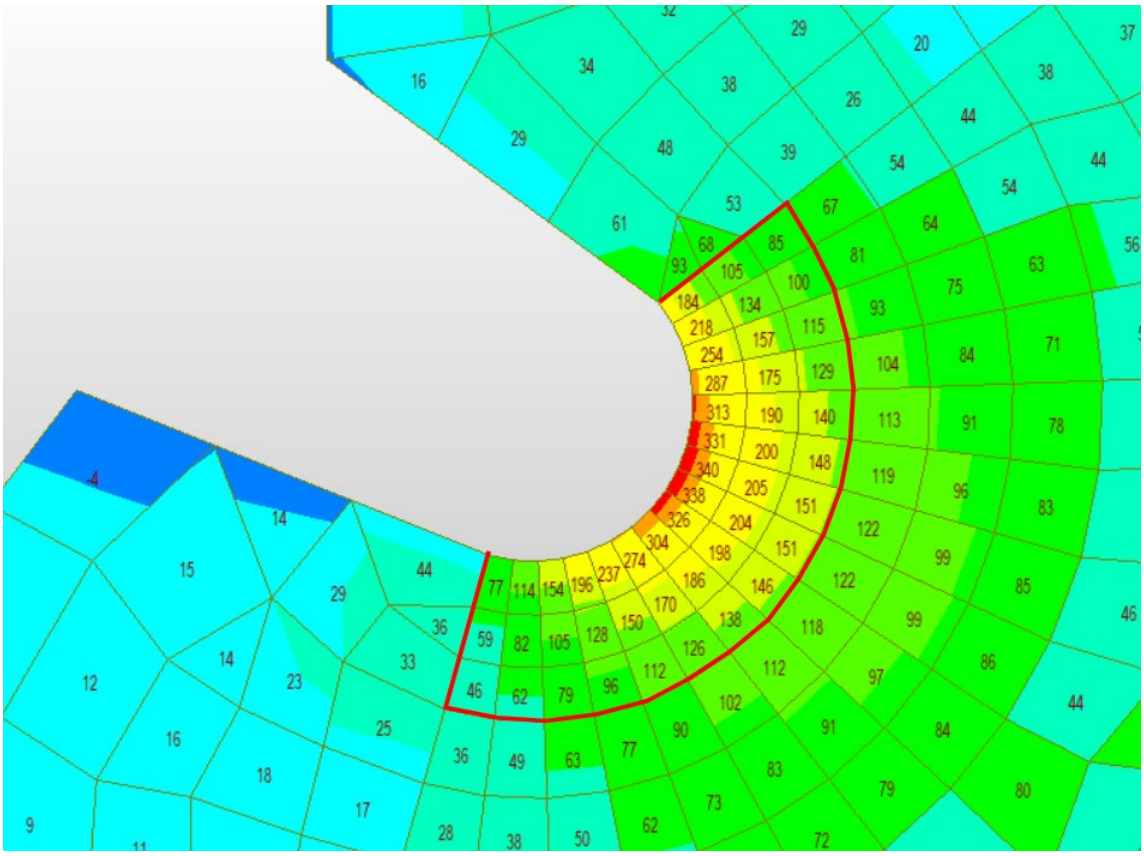

Figure 11. Gouge geometry, fatigue II maximum element local tangential stress range (MPa).

4.2.3 *Cantilever Span Web Taper Region Post Crack Arrest Hole Geometry*

The web taper corner is modeled with a gouge, crack at the tip of gouge, and 21mm (13/16") arrest hole centered approximately at the tip of crack. This model represents the geometry at the location with the web crack at the time of the MBI inspection. Larger arrest holes sized 51mm (2") and 102mm (4") (maintaining approximately the same depth of cut into the web at the edge) were also modeled to demonstrate how the larger radius holes affect the stress distribution around the arrest hole. All the arrest holes in these models were able to be meshed with a minimum of 40 elements (9 degrees between adjacent elements) around the hole to ensure the accuracy of stress concentrations. Figure 12 shows the 21mm (13/16") arrest hole geometry maximum element stresses for the fatigue II stress range due to the LRFD fatigue truck in the linear-elastic model. The red boundary in Figure 12 shows the location 6mm (¼") from the edge. This corresponds to the stress

in the fourth row of nodes, and the sixth row of nodes corresponds to the stress range 13mm (½") from the edge.

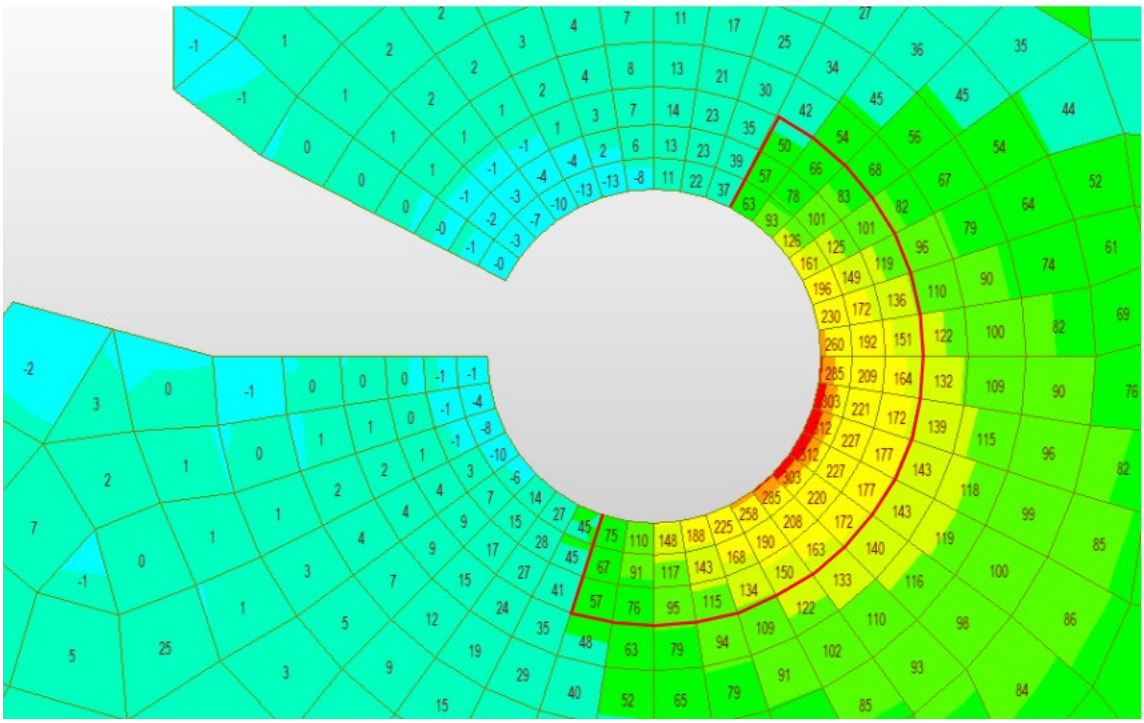

Figure 12. 21mm (13/16") Arrest hole geometry, fatigue II maximum element local tangential stress range (MPa).

4.2.4 *Cantilever Span Web Taper Region 4" Radius with Taper Geometry*

In this model the web taper corner is modeled with the entire corner removed and replaced with a smooth 102mm (4") radius transition. At the tangent ends of the radius an approximate 3-to-1 taper is used back to the edge of the web. This model represents an ideal repair at the location with the web crack. The radius is modeled with a 3-degree angle between adjacent elements increments. Figure 13 shows the 102mm (4") radius with taper geometry and maximum element stresses for the fatigue II stress range due to the LRFD fatigue truck in the linear-elastic model. Due to the amount of material removed in this repair detail, the maximum element edge stress shifts from the new radius edge to the edge of the nearest bolt hole. Although the edge stress is higher, the stress dissipates away from the bolt hole faster, and the 102mm (4") radius at 6mm (1/4") from the edge still controls the stress range. The red boundary in Figure 13 and Figure 14 shows the location 6mm (¼") from the edge for the radius and bolt hole, respectively. This corresponds to the stress in the second and third row of nodes (for the radius and bolt hole, respectively), and the third and fourth row of nodes (for the radius and bolt hole, respectively) correspond to the stress range 13mm (½") from the edge.

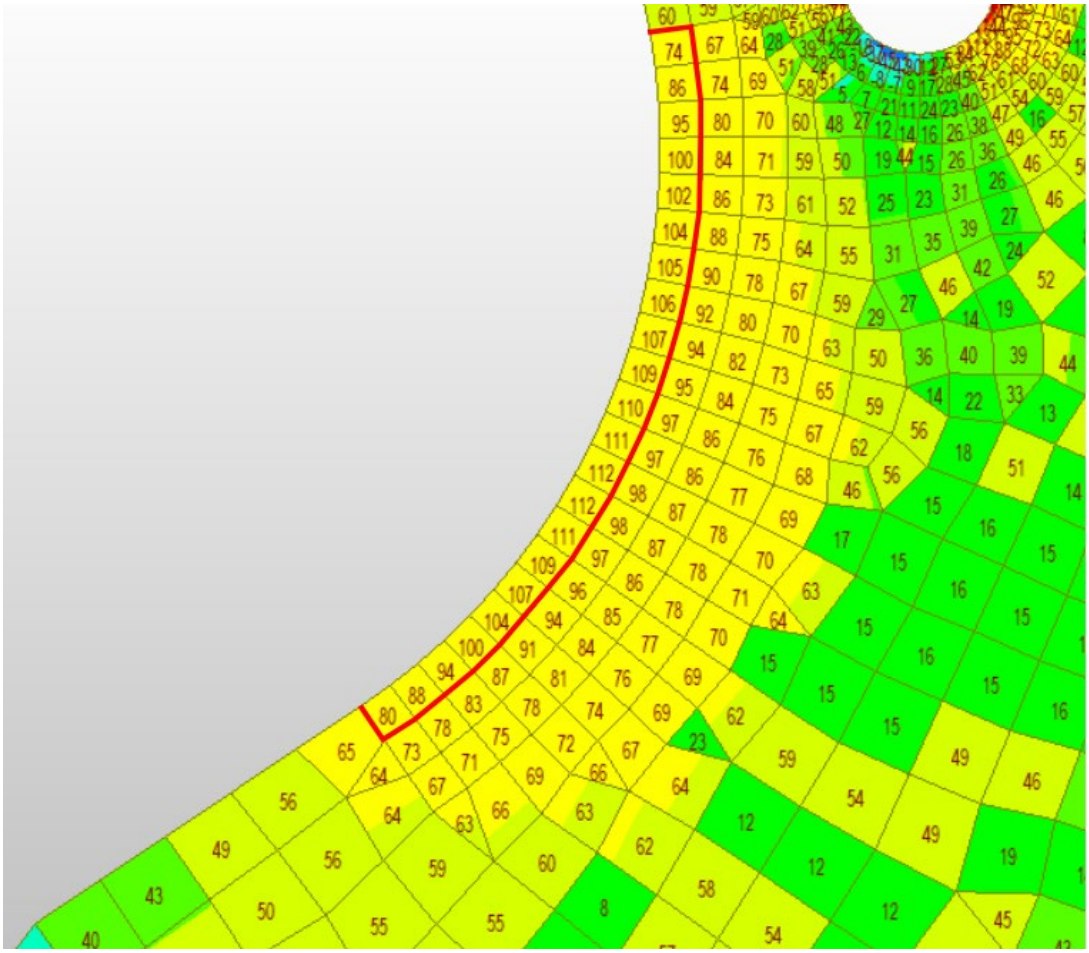

Figure 13. 102mm (4”) radius geometry, fatigue II max element local tangential stress range (MPa).

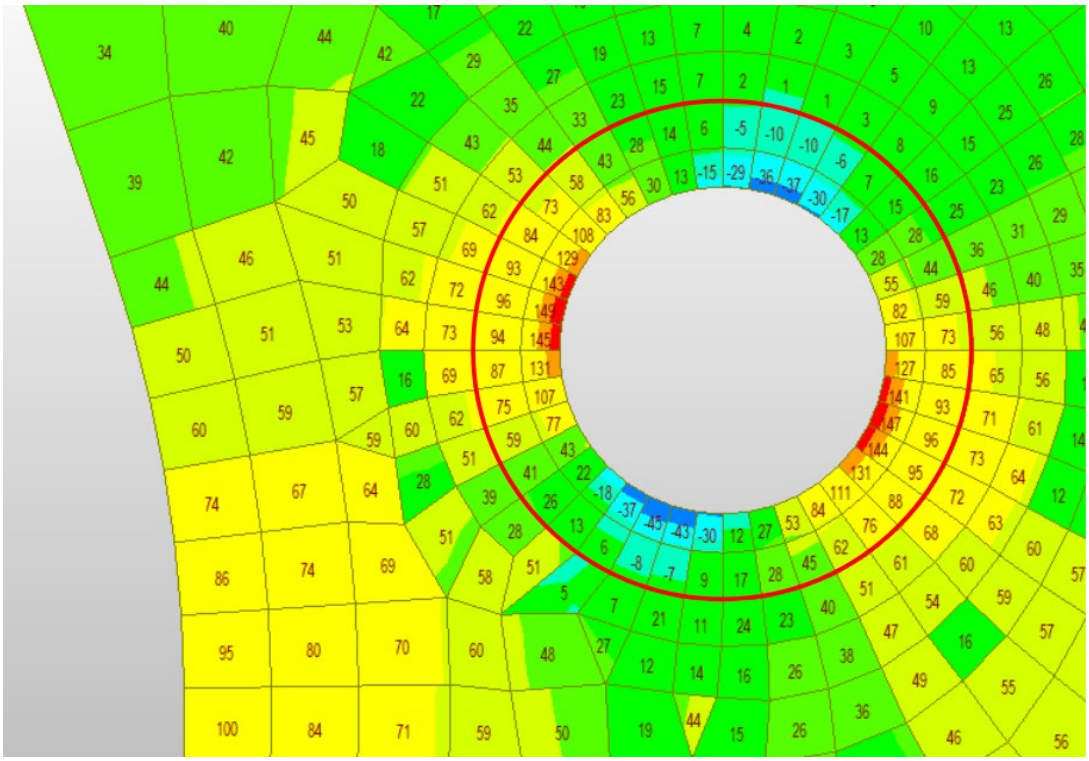

Figure 14. 102mm (4”) radius (at bolt hole), fatigue II max element local tangential stress range (MPa).

4.3 *Results Summary*

Because all stress ranges were so large, it was determined that the fatigue life of the original detail and any locations with flame-cut imperfections is exhausted (based on the 2019 AADT) and reprofiling and grinding of the edge is recommended to remove any existing microcracks and reset the fatigue life. Also, it was determined the fatigue life of the crack with arrest hole detail is not adequate when compared to the required additional service life of the bridge. Because of these discoveries, additional larger radius reprofiling repairs were investigated to determine improved repair details that would reduce fatigue stress ranges and increase fatigue life. It was determined that a profile with a 102mm (4") radius penetrating a maximum of 25mm (1") deep into the web from the original "As-designed" configuration would provide reduced stress ranges, but infinite life would not be achieved with reprofiling alone. Due to the depth of repair already completed at the location of the crack with arresting hole, reprofiling the edge of the web would also not provide adequate fatigue life.

Because an additional reduction in fatigue stress range was still required to achieve the minimum required fatigue life in these details, the addition of steel "strap" plates on one or both sides of the web was investigated. For this investigation, it was assumed strap plates would be added to the 102mm (4") radius reprofiled web repairs and at the single crack arrest hole location. The strap plate would use two of the three existing trough support bolt holes and require three new holes drilled below the web taper area and one above the trough support holes. Nine different strap plate configurations were investigated for each detail, which included a plate only on one side of the web vs both sides of the web, 6mm (¼") vs 13mm (½") vs 25mm (1") thick plates, and a longer strap, 350mm (14") between bolt holes vs a shorter strap, 200mm (8") between bolt holes. It was not possible to achieve infinite life with the single plate details because the single plate induced additional bending in the web increasing the stress on the outside of the web. Some single plate configurations did still increase the fatigue life of the repair. When strap plates were used on both sides of the web, the additional bending stress was eliminated, and the overall fatigue stress ranges were reduced as well. Many of the two plate configurations were able to achieve infinite life. See Figure 15 for an example of the reprofiled web with strap plates and Figure 16 for the crack arrest hole with strap plates. A summary of analyzed stress ranges and associated fatigue life is provided in Tables 2 through 4. In the tables Fatigue I stress ranges are multiplied by 1.75 and Fatigue II stress ranges are multiplied by 0.8. [1]

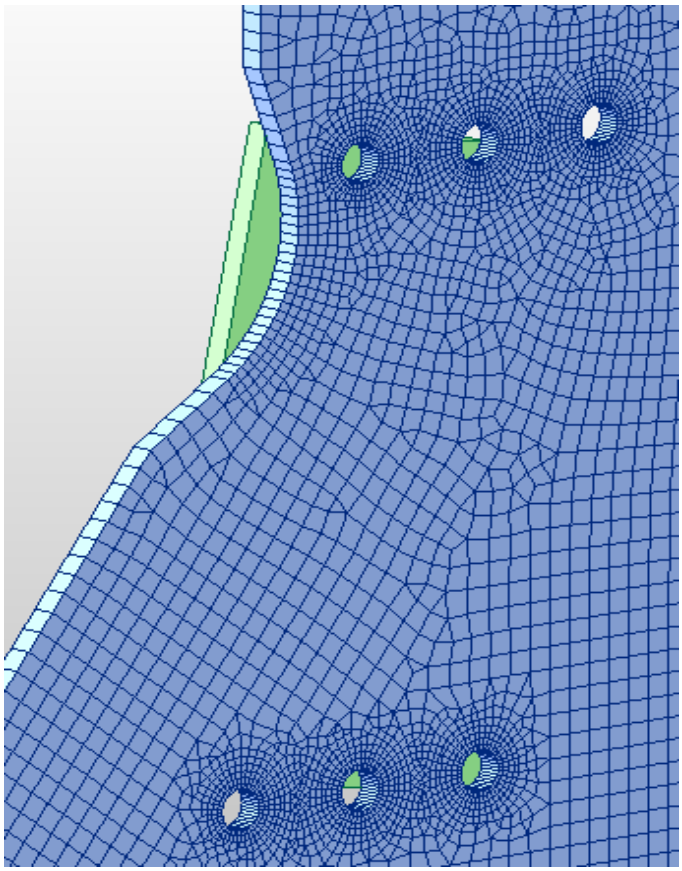

Figure 15. Typical 102mm (4”) radius reprofiled model with longer repair straps (front plate not shown).

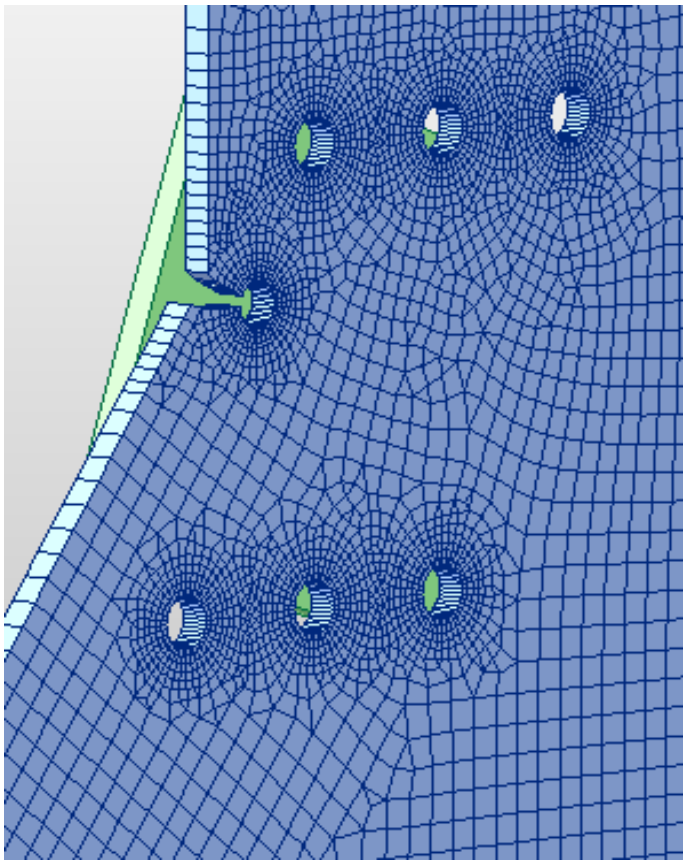

Figure 16. Crack with arrest hole model with shorter repair straps (front plate not shown).

Table 2. Web fatigue life comparison between design, damaged, and with web reprofiling geometries.

Load Rating Model	Fatigue I Stress Range (MPa)	Fatigue II Stress Range (MPa)	Fatigue II Stress Cycles (millions)	Fatigue II Life (years)
As-designed	211	87	12.5	8.2
Flame-cut with gouge (rad = 6mm)	273	112	5.8	3.8
Cracked with arrest hole	321	132	3.6	2.3
Larger arrest hole (rad =25mm)	308	127	4.0	2.6
Larger arrest hole (rad = 51mm)	274	113	5.7	3.7
Reprofile 25mm deep (rad = 102mm)	219	90	11.2	7.4
Reprofile 51mm deep (rad = 102mm)	236	97	9.0	5.9

Table 3. Web fatigue life comparison for crack with arrest hole with various repair plate configurations.

Load Rating Model	Fatigue I Stress Range (MPa)		Fatigue II Stress Range (MPa)		Fatigue II Stress Cycles (millions)		Fatigue II Life* (years)	
Side of Web	Left	Right	Left	Right	Left	Right	Left	Right
No plates added	321	321	132	132	3.6	3.6	2.3	2.3
13mm PL- RT side (350mm bolt spa)	338	213	139	88	3.1	12.2	2.0	8.0
25mm PL- RT side (350mm bolt spa)	302	214	124	88	4.3	12.0	2.8	7.9
13mm PL- RT side (200mm bolt spa)	321	163	132	67	3.6	27.0	2.3	INF
25mm PL- RT side (200mm bolt spa)	270	163	111	67	6.0	27.0	3.9	INF
13mm PL- both sides (350mm bolt spa)	188	188	77	77	17.7	17.7	11.6	11.6
25mm PL- both sides (350mm bolt spa)	157	157	65	65	30.3	30.3	INF	INF
6mm PL- both sides (200mm bolt spa)	177	177	73	73	21.1	21.1	13.9	13.9
13mm PL- both sides (200mm bolt spa)	137	137	56	56	45.5	45.5	INF	INF
25mm PL- both sides (200mm bolt spa)	106	106	44	44	97.7	97.7	INF	INF

*INF means infinite fatigue life met since Fatigue I stress range is below threshold.

Table 4. Web fatigue life comparison for combination reprofiling repair, 102mm (4”) radius up to 25mm (25mm) deep into base metal, with various repair plate configurations.

Load Rating Model	Fatigue I Stress Range (MPa)		Fatigue II Stress Range (MPa)		Fatigue II Stress Cycles (millions)		Fatigue II Life* (years)	
Side of Web	Left	Right	Left	Right	Left	Right	Left	Right
No plates added	219	219	90	90	11.2	11.2	7.4	7.4
13mm PL- RT side (350mm bolt spa)	234	156	96	64	9.1	31.2	6.0	INF
25mm PL- RT side (350mm bolt spa)	213	156	88	64	12.2	31.2	8.0	INF
13mm PL- RT side (200mm bolt spa)	220	129	91	53	11.0	54.2	7.2	INF
25mm PL- RT side (200mm bolt spa)	188	128	77	53	17.7	56.2	11.6	INF
13mm PL- both sides (350mm bolt spa)	140	140	58	58	42.6	42.6	INF	INF
25mm PL- both sides (350mm bolt spa)	120	120	49	49	67.7	67.7	INF	INF
6mm PL- both sides (200mm bolt spa)	133	133	55	55	50.5	50.5	INF	INF
13mm PL- both sides (200mm bolt spa)	106	106	44	44	97.7	97.7	INF	INF
25mm PL- both sides (200mm bolt spa)	102	102	42	42	111.7	111.7	INF	INF

*INF means infinite fatigue life met since Fatigue I stress range is below threshold.

5 STRENGTH EVALUATION

5.1 *Basis of Evaluation*

Using previous load rating files provided by IDOT, it was determined that the load rating of the bridge was not controlled by the shiplap connection in its as-designed configuration. However, there was desire to confirm this using more refined analysis. Also, there were concerns that cutting away portions of the web and drilling holes might reduce the strength capacity below the required level. This was also to be evaluated as part of this analysis. A finite element analysis (FEA) including material non-linearity was performed using Midas Civil software to compare with the shiplap connection rating from IDOT, which utilized hand calculations with AASHTO equations. The results showed general agreement between the two methodologies. Using the as-designed FEA model as the baseline, various conditions of the web region of the shiplap connection were modeled and analyzed using full incremental nonlinear analysis to determine whether the slight variations in geometry and additional bolt holes would affect the ultimate strength of the region.

5.2 *Modeling Details*

The same models from the fatigue evaluation (with the addition of an intermediate model with new bolt holes drilled into the web, but before steel strap plates are bolted on) were utilized for the strength evaluation (see Figure 17). While the full material properties of the steel were not relevant in the linear analysis, the material properties do play a large role in the nonlinear analysis. A majority of the web and flange steel is A441-50 (345 MPa) (High-Strength Low-Alloy Structural Manganese Vanadium Steel), specifically the web from the bearing support to the end of the cantilever for the finite element model. Lower stress portions of the web and flange steel are A373-32 (220 MPa) (Structural Steel for Welding), specifically the flanges and the web from the bearing support to the end of the finite element model. T-1 steel is also present in the web and flanges of the steel girders, but only in small regions at piers away from the shiplap connections.

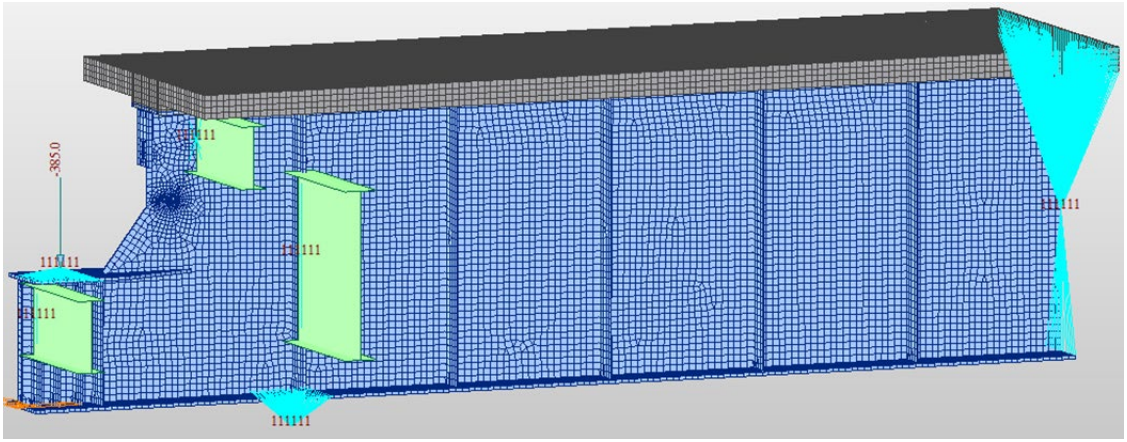

Figure 17. Cantilever span typical girder Midas Civil finite element model.

5.2.1 Mesh Size

For the nonlinear analysis, the mesh size was revised to 51mm x 51mm (2”x2”) elements since global behavior is being analyzed, and more refined models can lead to convergence issues. For the fatigue analysis, stress concentrations around the web taper area are the behavior being analyzed; therefore, in this area the maximum mesh size was kept to 13mm x 13mm (½”x ½”). Elements in areas around the bolt holes, gouges, or arrest holes can have much smaller elements and are needed to accurately analyze the stress fields. The mesh size away from the web taper area and over the majority of model remained as 51mm x 51mm (2”x2”) elements since further refinement was not necessary. Figure 18 shows the comparison in refinement in the web taper area for the nonlinear analysis model versus the fatigue analysis model.

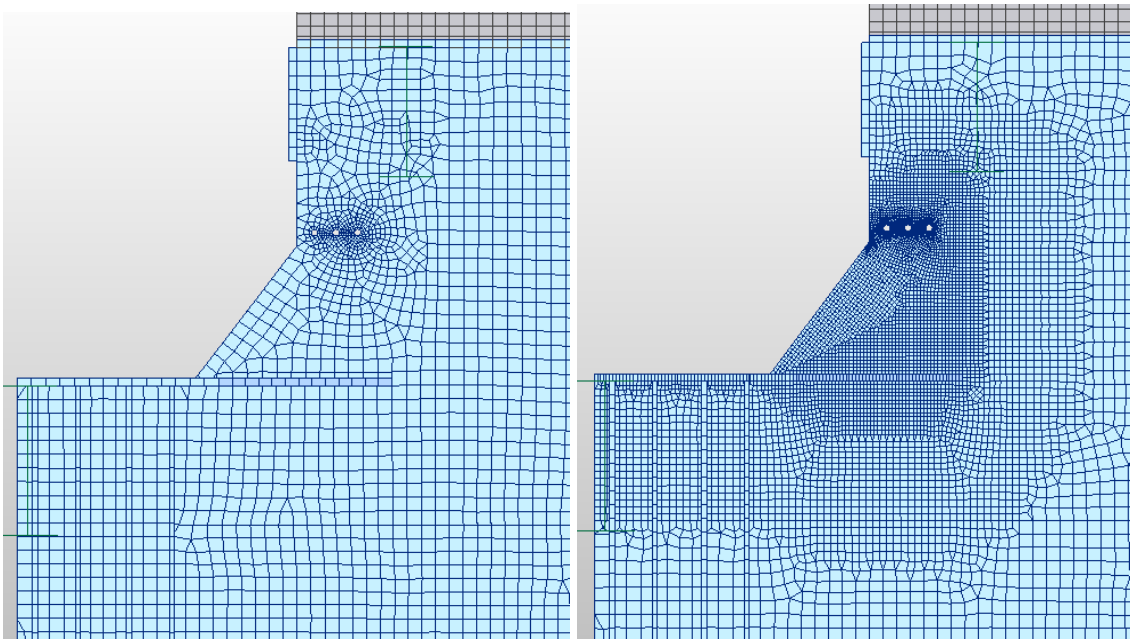

Figure 18. Mesh refinement for Ultimate Strength Analysis (left) and Fatigue Analysis (right).

Additional details about the nonlinear modeling techniques are listed below:

- The point load was applied at the center of the of the cantilever span rocker bearing updated to the dead load plus HS-20 live load reaction at the suspended span pin (extracted from the BrR model) factored for inventory level loading (1.3*D+2.17*L).
- All steel material was specified as a plastic material neglecting strain-hardening except regions with a concentrated load are specified with elastic material (76cm (30") width by 23cm (9") height of the web directly above the pier support bearings and bearing pad where loading is applied from the suspended span. This was necessary to improve model convergence).
- Material nonlinear analysis is performed utilizing the Newton-Raphson method incrementing the HS-20 inventory level load from 20% up to 100%+ to determine the ultimate capacity of the cantilever in the shiplap connection.
- Geometric nonlinear behavior was considered separately to account for any local instabilities that may occur, however, convergence issues did not allow for full material and geometric nonlinear analysis

5.3 *Results Summary*

The results of the full nonlinear FEA is best summarized by the global force-displacement curve at the applied load (see Figure 19). These curves show where the nonlinear response diverges from the linear response as well as the point of ultimate global instability. The modeling of the existing conditions (crack with arrest hole and flame-cutting gouge imperfections) produced similar ratings at the ultimate strength of this region as the as-designed model. Similarly, analysis with incremental web repair steps such as reprofiling of the web, the temporary state in which repair plate holes are drilled into the web (but plates are not bolted yet), and the final state for repair plates bolted on each side of the web produced similar ultimate loading results of the web region. As presented in Table 5, the removal of web material for the repair as well as drilling new holes and bolting of the repair plates indicated only a small reduction in capacity, defined as (ultimate load factor, ULF) * (inventory load, 1.3D+2.17L), from 1.40 to 1.30*(inventory load), which was still within an acceptable range. In other words, ULF indicates additional reserve capacity above the fully factored inventory loading applied in the model. The rating factors corresponding to the ultimate loads determined in the nonlinear analysis were calculated using MBE Eq. 6B.4.1-1, $RF=(C-A_1D)/(A_2L)$, where A_1 is equal to 1.3, A_2 is equal to 2.17 for inventory level rating & 1.3 for operating level rating, and capacity, C, is equal to (ULF)*(inventory load).

Figure 19. Load-deflection curve for model with crack with arrest hole linear and nonlinear analysis at top of cantilever end.

Table 5. Load rating comparison

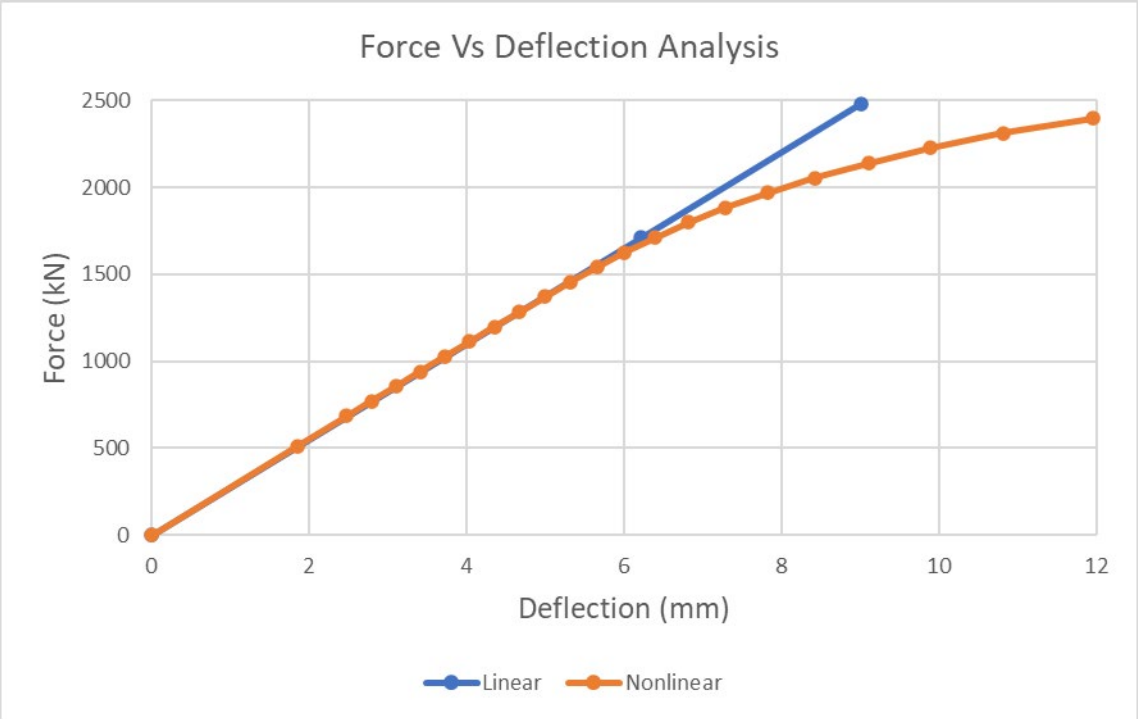

Load Rating Model	ULF*	INV RF	OPR RF
IDOT BrR Girder Rating (Controlling)	N/A	0.88	1.47
IDOT Hand Calculation for Shiplap	N/A	1.36	2.27
FEA with Arrest hole - no new bolt holes or PLs	1.40	1.73	2.90
FEA with Arrest hole - new bolt holes, no PLs	1.30	1.55	2.59
FEA with Arrest hole - new bolt holes and PLs	1.40	1.73	2.90
FEA with 102mm (4") rad reprofile - no new bolt holes or PLs	1.40	1.73	2.90
FEA with 102mm (4") rad reprofile - new bolt holes, no PLs	1.30	1.55	2.59
FEA with 102mm (4") rad reprofile - new bolt holes and PLs	1.40	1.73	2.90

*ULF stand for ultimate load factor from the FEA as compared to factored INV loading (1.3D+2.17L) from nonlinear analysis

5.3.1 *Stress Analysis Results*

The stresses throughout the tapered web region for the model with the crack and arrest hole throughout the web modifications are shown in shown in Figures 20 through 22. The figures represent the stress state at the final converging step in the material non-linear analysis results and show how force distribution changes throughout the web but still reaches a similar ultimate capacity. Note that "x" in Figures 20 through 22 represent local web steel yielding and redistribution of forces.

The FEA stress contours for the web plate at the ultimate loading indicate that the stress field is being interrupted by the arresting hole and bolt holes and localized stresses above yield do occur. However, plastic stress redistribution allows for further strength to be developed beyond point of first yield. The strap plates and bolts were included in the FEA models, but they were not designed like a typical splice plate would be because their main purpose is stiffening to reduce fatigue stress ranges in the web and not strengthening. These plates are not needed to increase the ultimate strength of the shiplap connection and therefore they are allowed to slip and yield, which is accounted for in the nonlinear FEA model. Also, these bolts and plates will only see vehicular live load and were designed to withstand Inventory level HS-20 loading. The rating for the shiplap connection remains higher than the controlling location of the bridge (from BrR) throughout the repair process, therefore no special restrictions are needed.

Figure 20. Stress state at ultimate from material non-linear analysis for arrest hole geometry (MPa).

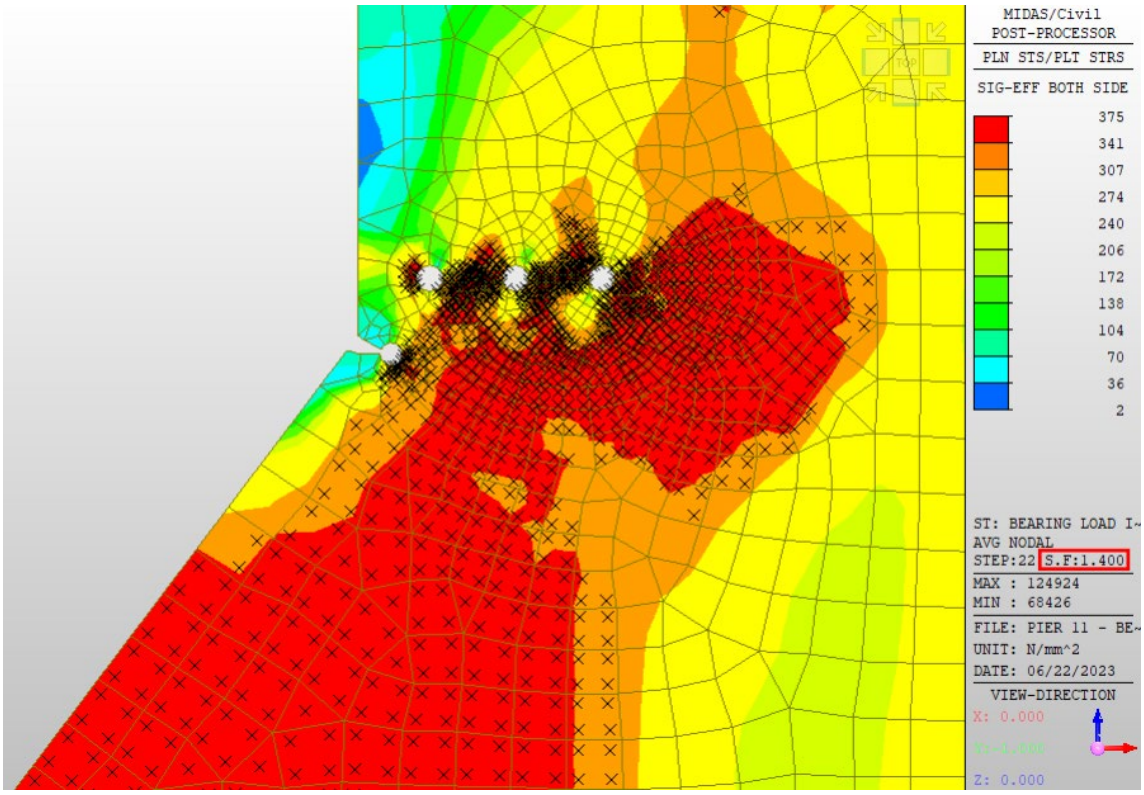

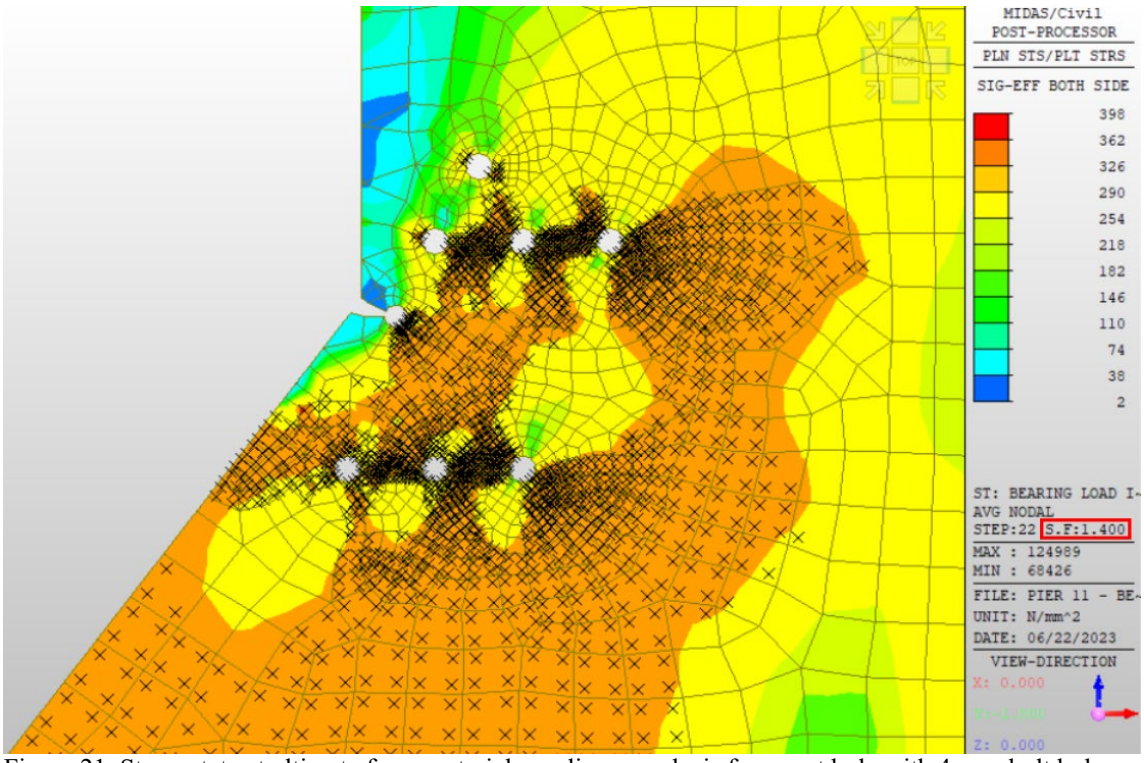

Figure 21. Stress state at ultimate from material non-linear analysis for arrest hole with 4 new bolt holes (MPa).

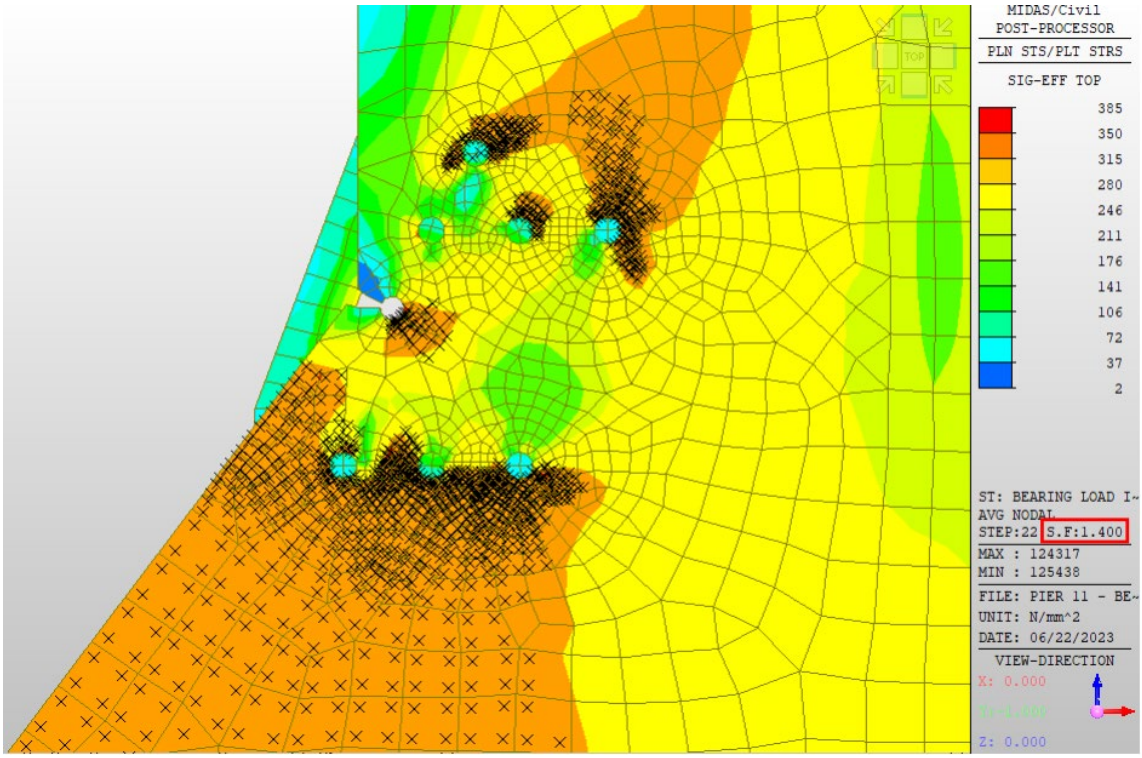

Figure 22. Stress state at ultimate from material non-linear analysis for arrest hole with 4 new bolt holes and repair plates (front plate not shown for clarity) (MPa).

5.3.2 *Buckling Analysis Results*

To investigate the potential for local buckling to reduce the ultimate strength of the shiplap connection, a linear buckling analysis was performed which considered the first 20 potential buckling modes. Buckling analysis requires the user to review each mode shape and determine which mode(s) are applicable to the response of interest. Buckling mode 12 was found to be most applicable to the cantilever region, which represents local web buckling between the bearing stiffeners and end of cantilever (see Figure 23). This buckling mode could be considered as a form of web bend buckling from the cantilever moment; however it is subjected to a complex stress state which includes shear from the cantilever and vertical compression from the concentrated reaction force as well.

The critical load factor for this mode was determined to be 3.2, which means that buckling would be predicted at this value times the applied load. The model for this analysis was loaded with the factored LFD inventory load of 1713kN (385kips) obtained from the AASHTOWare BrR model. This mode represents a critical load of approximately 3.2*1713=5482kN (1232kips) where 1713kN (385kips) comes from the LFR Inventory HS20 loading. With such a high critical load (2.28 times the ultimate load from the nonlinear analysis), it was concluded that buckling would not create a meaningful reduction of the ultimate strength.

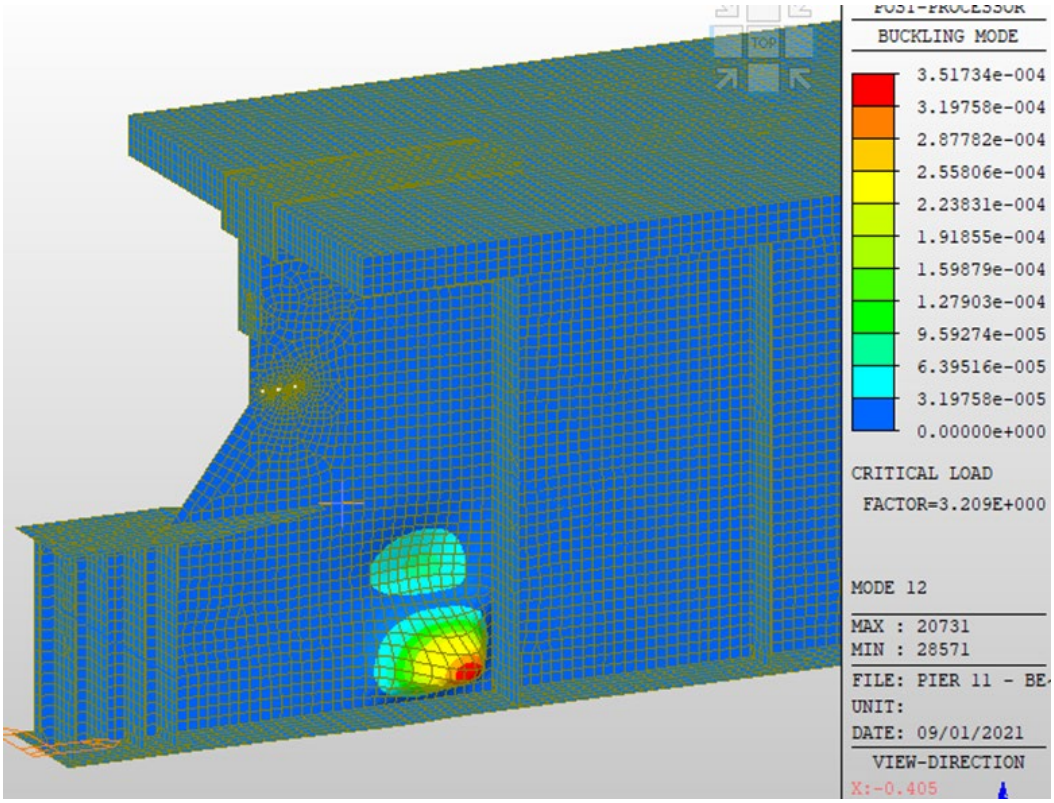

Figure 23. Lowest applicable cantilever girder end region buckling mode and critical load factor.

Buckling analysis was also performed on the suspended span girder end region. In this case, the lowest applicable critical load factor in the support web panel was found to be 1.6, which translates to a critical load of 1.6*1713=2741kN (616 kips) where 1713kN (385kips) represents the LFR Inventory HS20 loading. This mode corresponds to shear buckling of the web, which will be captured by the AASHTOWare BrR load rating code check. No further investigation was deemed necessary.

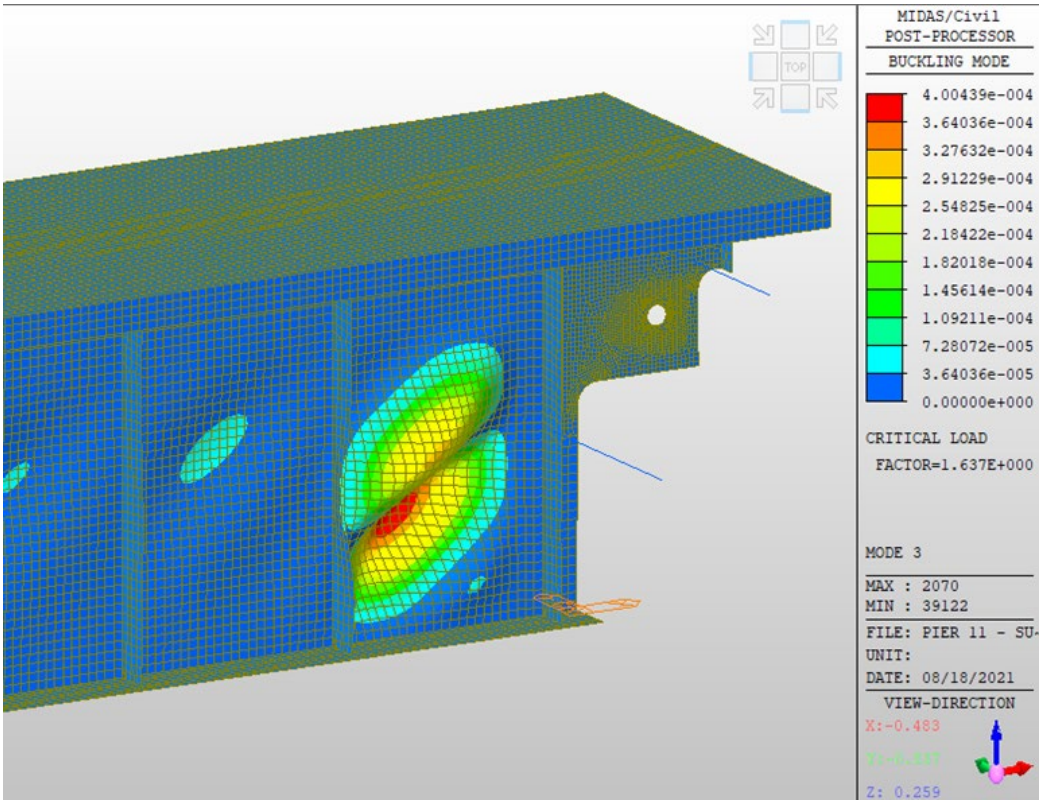

Figure 24. Lowest applicable suspended span girder end region buckling mode and critical load factor.

6 CONCLUSION

In this project, IDOT was faced with a very difficult challenge. This aging steel bridge with unique design and T-1 steel was discovered to have fatigue cracking in a connection of a non-redundant steel tension member, and the initial analyses based on refined three-dimensional finite element analysis indicated fully exhausted fatigue life with additional cracking expected. However, the bridge was programmed for near term replacement and any repairs might disrupt traffic on a heavily traveled interstate roadway. MBI and IDOT worked together to develop an innovative and cost-effective solution to protect the bridge against further cracking without disruption to the traveling public. Repairs included reprofiling the web free edge and adding supplemental bolted strap plates to reduce fatigue stresses and achieve infinite life. Load rating analysis using full nonlinear FEA was also performed on the existing connection and with retrofits applied to verify capacity. These repairs were performed at 11 locations by IDOT skilled maintenance labor in 2022 without any significant issues.

REFERENCES

[1] AASHTO. AASHTO LRFD Bridge Design Specifications. 9th Edition. Washington, DC: American Association of State Highway and Transportation Officials. 2020.

[2] AASHTO. Manual for Bridge Evaluation. 3rd Edition. Washington, DC: American Association of State Highway and Transportation Officials. 2017.

[3] Russo, F., D. Mertz, K. Frank, K. Wilson. Design and Evaluation of Steel Bridges for Fatigue and Fracture – Reference Manual. FHWA-NHI-16-016, Washington, DC: Federal Highway Administration. 2016.

[4] Connor, R., J. Fisher, W. Gatti, V. Gopalaratnam, B. Kozy, B. Leshko, D.L. McQuaid, R., Medlock, D. Mertz, T. Murphy, D. Paterson, O. Sorensen, and J. Yadlosky. Manual for Design, Construction, and Maintenance of Orthotropic Steel Deck Bridges. FHWA-IF-12-027, Washington, DC: Federal Highway Administration. 2012